Neuron, Vol. 30, 135–147, April, 2001, Copyright ©2001 by Cell Press

Deregulation of Cdk5 in a Mouse Model of ALS: Toxicity Alleviated by Perikaryal Neurofilament Inclusions

Minh Dang Nguyen, Roxanne C. Larivière, and Jean-Pierre Julien*
Centre for Research in Neurosciences
McGill University
Research Institute of the McGill University Health Centre
Montréal, Québec, H3G 1A4
Canada

Summary

Recent studies suggest that increased activity of cyclin-dependent kinase 5 (Cdk5) may contribute to neuronal death and cytoskeletal abnormalities in Alzheimer's disease. We report here such deregulation of Cdk5 activity associated with the hyperphosphorylation of tau and neurofilament (NF) proteins in mice expressing a mutant superoxide dismutase (*SOD1^{G37R}*) linked to amyotrophic lateral sclerosis (ALS). A Cdk5 involvement in motor neuron degeneration is supported by our analysis of three *SOD1^{G37R}* mouse lines exhibiting perikaryal inclusions of NF proteins. Our results suggest that perikaryal accumulations of NF proteins in motor neurons may alleviate ALS pathogenesis by acting as a phosphorylation sink for Cdk5 activity, thereby reducing the detrimental hyperphosphorylation of tau and other neuronal substrates.

Introduction

Amyotrophic lateral sclerosis (ALS) is an adult-onset neurological disorder characterized by the selective degeneration of motor neurons leading to paralysis and death within 3–5 years (for review, see Cleveland, 1999; Julien, 2001). Missense mutations in the gene coding for the Cu/Zn superoxide dismutase 1 (SOD1), located on chromosome 21, account for ~20% cases of familial ALS (Rosen et al., 1993; Cudkowicz et al., 1997). The SOD1 protein is a cytosolic metalloenzyme catalyzing the conversion of superoxide anions to hydrogen peroxide (Fridovich, 1986). Transgenic mice expressing mutant SOD1 develop motor neuron disease resembling ALS through a gain of unidentified deleterious properties (Wong et al., 1995; Bruijn et al., 1997, Bruijn et al., 1998). Several mechanisms have been proposed to account for such toxicity, including excitotoxicity (Bruijn et al., 1997; Trotti et al., 1998), oxidation/nitration-related damage (Beckman et al., 1993; Wideau-Pazos et al., 1996), disruption of the calcium homeostasis (Morrison et al., 1996; Roy et al., 1998), copper toxicity (Corson et al., 1998), apoptosis mediated by caspases activation (Pasinelli et al., 1998; Li et al., 2000), and zinc deficiency (Estevez et al., 1999).

Abnormal accumulations of neurofilaments (NFs) in the perikaryon or axon of spinal motor neurons have been observed in ALS patients (Carpenter, 1968; Hirano et al., 1984; Schmidt et al., 1987; Rouleau et al., 1996) and in mice overexpressing ALS-linked SOD1 mutants (Wong et al., 1995; Bruijn et al., 1997). It remains unknown to what extent NF abnormalities contribute to the pathogenesis of human ALS, but recent transgenic mouse studies suggest that an axonal localization of intermediate filament aggregates may be an important factor of toxicity (Williamson et al., 1998; Beaulieu et al., 1999; Beaulieu et al., 2000). The overexpression in mice of wild-type NF subunits can provoke ALS-like NF accumulations in the perikaryon of motor neurons, axonal atrophy, and sometimes motor dysfunction caused by altered ionic conductances, but it does not cause massive motor neuron death (for review, see Julien, 1999). Remarkably, the overexpression of human NF heavy subunits (NF-H) increased by up to 65% the life span of mice expressing *SOD1^{G37R}*, suggesting a protective effect of perikaryal accumulations of NF proteins (Couillard-Després et al., 1998). The NF-H protein is a highly phosphorylated protein, and its KSP (Lys-Ser-Pro) repeat-enriched tail domain constitutes a target for several protein kinases, including stress-activated protein kinase-γ (SAPK-γ) (Giasson and Mushynski,1996), extracellular signal regulated kinases (ERK 1/2) (Veeranna et al., 1998), glycogen synthase kinase 3 (GSK-3) (Guidato et al., 1996; Bajaj and Miller, 1997), and cyclin-dependent kinase 5 (Cdk5), a serine/threonine kinase with close structural homology to the mitotic cyclin-dependent kinases (Cdk) (Guidato et al., 1996; Bajaj and Miller, 1997; Bajaj et al., 1999).

Activation of Cdk5 requires critical association with its neuron-specific regulatory subunit p35 (Tsai et al., 1994). The p35/Cdk5 complex is essential for central nervous system development and mainly for neurite outgrowth (Tsai et al., 1993; Nikolic et al., 1996; Oshima et al., 1996; Kwon and Tsai, 1998). In addition to NF-H, the substrates for Cdk5 include the microtubule-associated protein tau, Munc-18, DARPP-32, the Retinoblastoma protein, PAK1, Synapsin 1, c-src, and APC (Mandelkow, 1999). The abnormal subcellular localization of Cdk5 has been observed in several neurodegenerative diseases, including ALS (Bajaj et al., 1998), Alzheimer's disease (Yamaguchi et al., 1996; Pei et al., 1998), Parkinson's disease (Brion and Couck, 1995), as well as canine motor neuron disease (Green et al., 1998). Moreover, recent studies suggest that a deregulation of Cdk5 activity may directly contribute to pathogenesis. Patrick et al. (1999) reported the accumulation of p25, a truncated form of p35, in the brains of patients with Alzheimer's disease. Their results show that p25, which is not targeted to the plasma membrane like p35, sequesters Cdk5 away from normal compartments of p35/Cdk5 and deregulates its activity. Expression of the p25/Cdk5 complex in cultured cortical neurons induced cytoskeletal abnormalities and apoptosis (Patrick et al., 1999; Lee et al., 2000). Moreover, the overexpression of p25 in the CNS of transgenic mice caused hyperphosphorylation of tau and NFs, cytoskeletal disruption, and behavioral deficits (Ahlijanian et al., 2000).

*To whom correspondence should be addressed (e-mail: mdju@musica.mcgill.ca).

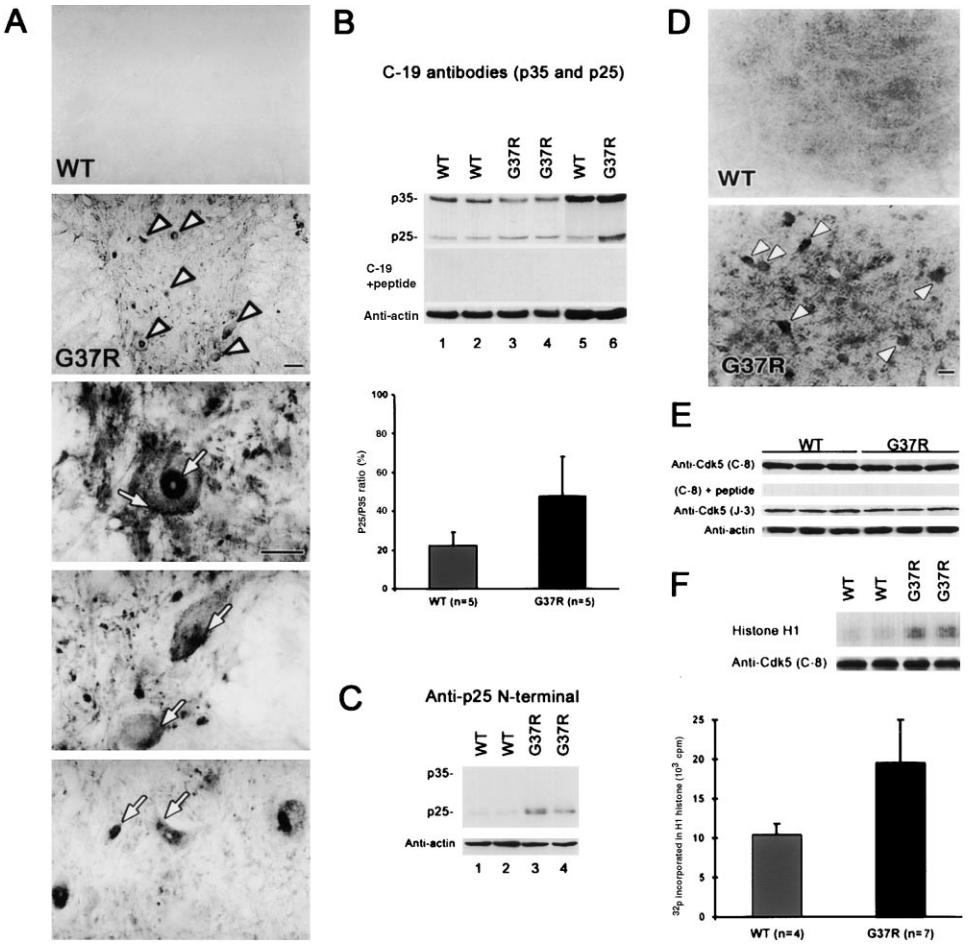

Figure 1. P25-Dependent Mislocalization and Deregulation of Cdk5 in Spinal Motor Neurons of *SOD1*^{G37R} Mice

(A) Immunoreactivity for Cdk5 occurs at the cell membrane and in the cell body and nucleus of spinal motor neurons in ventral horn of *SOD1*^{G37R} mice (*G37R*) (second panel, white arrowheads, and last three panels, white arrows), whereas Cdk5 immunostaining in spinal motor neurons of normal mice (WT) is extensively reduced (first panel). Bars, 20 μm (two upper panels) and 15 μm (three lower panels).

(B) Western blots of total extracts (lanes 1 to 4) or soluble extracts (lanes 5 and 6) of spinal cord from *SOD1*^{G37R} and normal mice with an antibody recognizing both p25 and p35 (C-19) revealed an increased p25/p35 ratio in *SOD1*^{G37R} mice as compared with normal mice. The blots were stripped and incubated with anti-actin antibodies. The levels of the protein are similar in the different samples. Quantitative analysis by densitometry with the C-19 antibodies showed elevated p25/p35 ratios (up to 70%) in *SOD1*^{G37R} mice, whereas it is of ~20% in normal mice.

(C) Western blots of soluble extracts of spinal cord from normal and *SOD1*^{G37R} mice with an antibody recognizing p25 (N-23) show enhanced levels of p25 protein level in *SOD1*^{G37R} mice as compared with normal mice. The N-23 antibodies recognizing specifically the N terminus of p25 but not p35 yielded very poor p25 signal in samples from normal mice (WT) in contrast to samples from *SOD1*^{G37R} mice.

(D) Immunohistochemical staining with N-23 antibodies confirmed the presence of p25 in motor neurons of *SOD1*^{G37R} mice (white arrowheads). Bar, 20 μm.

(E) Western blots with two Cdk5 antibodies (C-8 and J-3) reveal unchanged levels of the Cdk5 kinase in *SOD1*^{G37R} mice despite its mislocalization in spinal motor neurons. The specificity of C-8 antibodies was confirmed with the preincubation of antibodies with a Cdk5 peptide.

(F) Kinase assays performed after immunoprecipitation of spinal cord extracts with Cdk5 antibodies showed a 2-fold increase in total specific kinase activity of Cdk5 from the spinal cord of *SOD1*^{G37R} mice. Autoradiogram showing the quantity of ^{32}P incorporated in histone H1 from Cdk5 in spinal cord extracts of normal and *SOD1*^{G37R} mice (upper panel). The lower panel shows the immunodetection of Cdk5. The histograms show the quantification of ^{32}P after correction for Cdk5 protein levels. All immunohistochemistry, Western blot, and kinase assay experiments were carried out with 8- to 12-month-old *SOD1*^{G37R} mice and age-matched normal littermates.

We report here that the p25/p35 ratio and Cdk5 activity are abnormally elevated in the spinal cord of transgenic mice expressing *SOD1*^{G37R} and that this is associated with the hyperphosphorylation of NF and tau proteins. There was a slowing down of disease in three *SOD1*^{G37R} mouse lines exhibiting abnormal accumulations of NF proteins in perikarya of motor neurons. We propose that perikaryal NF accumulations may act as a phosphorylation sink for deregulated Cdk5 activity in ALS mice, thereby reducing the noxious hyperphosphorylation of tau and other cellular substrates.

Results

High p25/p35 Ratio and Deregulated Cdk5 Activity in *SOD1*^{G37R} Mice

To investigate the potential involvement of kinases in disease caused by mutant SOD1, we have compared

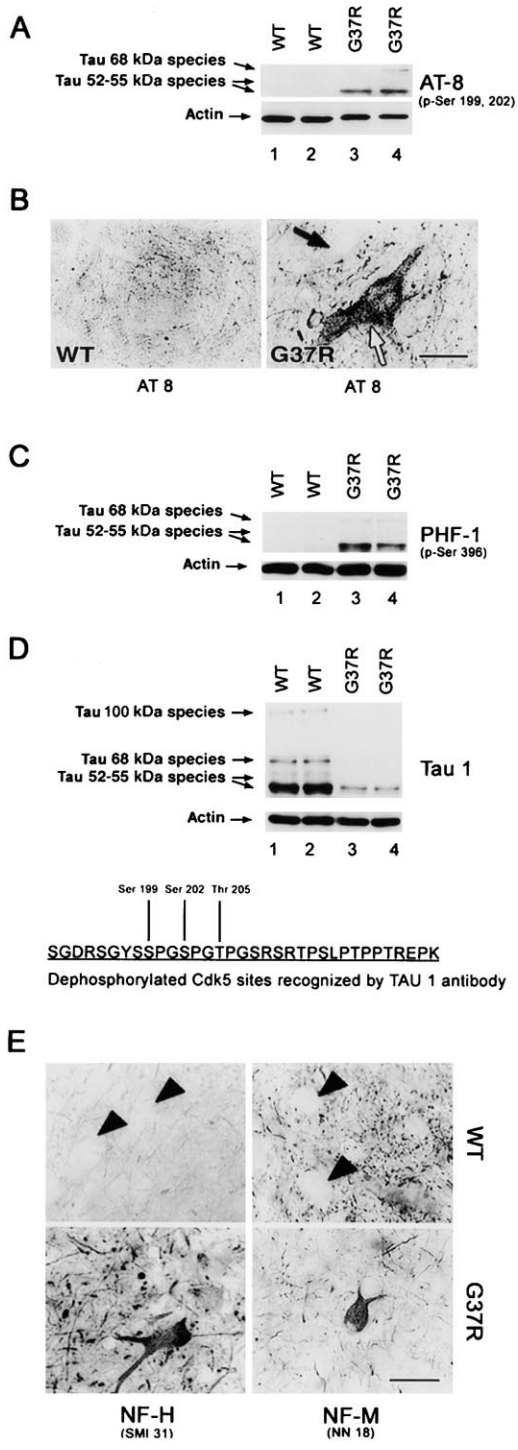

Figure 2. Hyperphosphorylation of Tau and NF Proteins in Motor Neurons of *SOD1*^{G37R} Mice

(A) A Western blot of spinal cord extracts shows the hyperphosphorylation of tau at Cdk5 sites (serines 199 and 202).

(B) Immunohistochemical staining with the monoclonal antibody AT-8 confirmed that tau is hyperphosphorylated in some motor neurons of *SOD1*^{G37R} mice (white arrow). Note that not all motor neurons exhibited an AT8-positive signal (black arrow). Bar, 15 μm.

(C) A Western blot of spinal cord extracts shows the hyperphosphorylation of tau at one other Cdk5 site (serine 396) in *SOD1*^{G37R} mice (*G37R*) (lanes 3 and 4) as revealed by PHF-1 immunoreactivity, unlike extracts from normal mice (WT) (lanes 1 and 2).

by immunohistochemistry the distribution of various kinases in the spinal cord of *SOD1*^{G37R} mice (line 29) and of normal mice. Phospho-dependent antibodies recognizing activated or inactivated forms of MEK1/2, Erk1/2, JNK, p38, Gsk-3β, and p70S6K did not reveal major immunostaining differences in spinal motor neurons between *SOD1*^{G37R} mice and normal mice (data not shown). However, activated forms of Erk1/2, p38, and p70S6K were detected in glial cells of *SOD1*^{G37R} mice (data not shown). In contrast, a striking difference was observed in the immunostaining of motor neurons with antibodies against Cdk5. In normal mice, anti-Cdk5 antibodies yielded very poor immunoreactivity in the cell body of spinal motor neurons (Figure 1A, upper panel), whereas an intense Cdk5 immunostaining was observed in spinal motor neurons of *SOD1*^{G37R} mice (Figure 1A, second panel, white arrowheads). Moreover, whereas Cdk5 is normally targeted to the cell membrane (Patrick et al., 1999), the Cdk5 in *SOD1*^{G37R} mice was detected in the cytoplasm and nucleus of motor neurons (Figure 1A, last three panels, white arrows). Such mislocalization of Cdk5 in neurons has been previously attributed to the conversion of p35 to p25, which lacks the conserved myristoylation sequence of p35 (Patrick et al., 1999).

Using an antibody (C-19) recognizing both the p25 and p35 fragments, we have determined by Western blotting the p25 and p35 levels in spinal cord extracts from normal mice and from *SOD1*^{G37R} mice (Figure 1B). The p25/p35 ratio in total spinal cord extracts from *SOD1*^{G37R} mice was higher than those from normal mouse littermates (Figure 1B, lanes 1–4). The increase of p25/p35 ratio in *SOD1*^{G37R} mice was even more pronounced in soluble spinal cord extracts (Figures 1B, lanes 5 and 6). Quantitative analysis of the band signals from the soluble fraction using the ImageQuant and Gel Pro Analyzer software revealed a 3-fold increase of p25/p35 ratio in *SOD1*^{G37R} mice as compared with normal littermates (Figure 1B). The increase of p25 protein levels in *SOD1*^{G37R} mice was further confirmed by Western blots with an antibody recognizing specifically the N terminus of p25 but not p35 (Figure 1C). Immunostaining of spinal cord sections from *SOD1*^{G37R} mice with an anti-p25 N-terminal antibody further confirmed the presence of p25 in spinal motor neurons (Figure 1D). These results suggest that p25 is likely responsible for the mislocalization of Cdk5 in motor neurons of *SOD1*^{G37R} mice. Note that in spite of its mislocalization, the levels of Cdk5 protein in the spinal cord of *SOD1*^{G37R} mice remained similar to those in normal mice, as revealed by immunoblotting with polyclonal C-8 and monoclonal J-3 antibodies (Figure 1E). Preincubation of C-8 antibodies with a Cdk5 blocking peptide abolished the immunoreactivity for Cdk5. To determine whether the high p25/p35 ratio was associated with enhanced Cdk5 kinase activity, Cdk5 was im-

(D) A Western blot of spinal cord extracts shows the hyperphosphorylation of tau at Cdk5 sites in *SOD1*^{G37R} mice (lanes 3 and 4), as revealed by the reduced Tau 1 immunoreactivities as compared with extracts of normal mice (lanes 1 and 2).

(E) Immunohistochemistry demonstrates the abnormal hyperphosphorylation of NF-M and NF-H proteins in the neuronal perikarya of *SOD1*^{G37R} mice. The black arrowheads point to cell bodies in the spinal cord of normal mice. Bar, 10 μm.

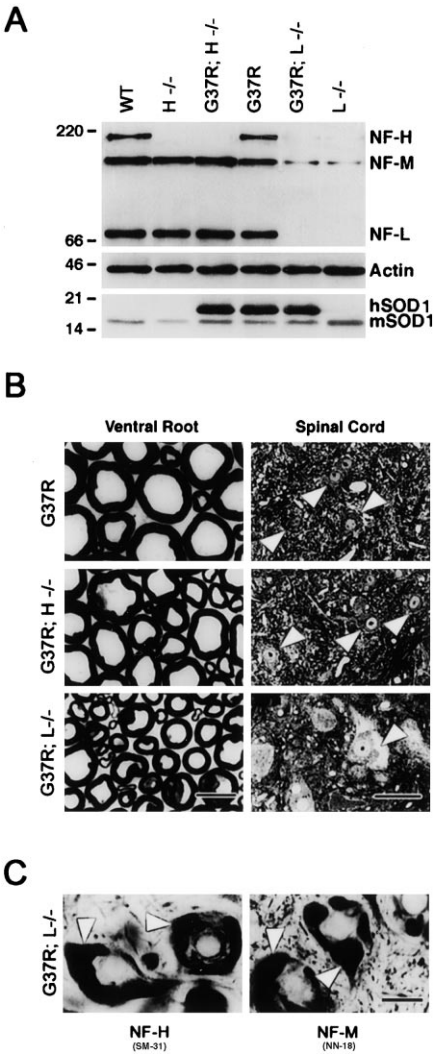

Figure 3. Perikaryal Accumulations of NF Proteins in *SOD1*^{G37R} Mice Lacking NF-L

(A) NF and SOD1 protein expression in mice knockout for NF-H or NF-L genes. Western blot analysis of spinal cord extracts from 7-month-old mice confirms the absence of NF-H and NF-L in mice with disrupted NF-H or NF-L genes, respectively. The RT-97 and NR-4 antibodies were used for the immunodetection of NF-H and NF-L, respectively. No changes in levels of NF-L protein occurred in NF-H null mice (*H*$^{-/-}$ and *G37R;H*$^{-/-}$ mice), whereas a 90% reduction of NF-H and NF-M protein levels occurred in NF-L null mice (*L*$^{-/-}$ and *G37R;L*$^{-/-}$) mice. The lack of NF-H or NF-L did not affect levels of endogenous wild-type (mSOD1) or human *SOD1*^{G37R} proteins.

(B) Transverse sections of L5 ventral roots and spinal cord from *SOD1*^{G37R} mice, *SOD1*^{G37R} lacking NF-H (*G37R;H*$^{-/-}$), and *SOD1*^{G37R} mice lacking NF-L (*G37R;L*$^{-/-}$). All mice were at 4 months old at a stage in which there are no signs of degeneration. The lack of NF-H had few effects on the radial growth of motor axons, whereas the absence of NF-L resulted in a dramatic decrease of axonal caliber. Moreover, the *SOD1*^{G37R} mice lacking NF-L exhibited accumulations in the perikaryon of spinal motor neurons (white arrowheads), unlike spinal motor neurons of *SOD1*^{G37R} mice with a normal NF background (white arrowheads) or lacking NF-H (white arrowheads). Bars, 7 μm (left panel) and 25 μm (right panel).

(C) Immunodetection of NF proteins in neuronal perikarya of *SOD1*^{G37R} mice lacking NF-L. Immunostaining of spinal cord sections from *G37R;L*$^{-/-}$ mice revealed intense SMI 31 and NN-18 immunoreactivities (white arrowheads). These antibodies recognize phosphorylated NF-H and NF-M, respectively. This staining indicates that perikaryal inclusions in spinal motor neurons of *G37R;L*$^{-/-}$ mice are made up with phosphorylated NF-H and NF-M. Bar, 30 μm.

munoprecipitated with anti-Cdk5 antibodies from spinal cord lysates (250 μg) followed by a kinase assay using histone H1 as exogenous substrate. Figure 1F (upper gel) shows an autoradiogram of ^{32}P-labeled histone H1 using Cdk5 from spinal cord extracts of normal and *SOD1*^{G37R} mice. The lower panel in figure 1F shows the detection of immunoprecipitated Cdk5 with C-8 antibodies. Quantification of radioactivity incorporated in histone H1 was performed by phosphoimager and adjusted to the level of Cdk5 immunoprecipitated. Our analysis revealed a 2-fold increase of specific Cdk5 kinase activity in lysates of *SOD1*^{G37R} mice (8–12 months old) as compared with age-matched normal littermates (histogram in Figure 1F).

Hyperphosphorylation of Tau and NF Proteins in *SOD1*^{G37R} Mice

We then examined whether the increased Cdk5 activity in *SOD1*^{G37R} mice was associated with hyperphosphorylation of Cdk5 cytoskeletal substrates such as tau and NF proteins. We used the AT-8 and PHF-1 antibodies that recognize three phosphoserines (199, 202 for AT-8, and 396 for PHF-1) in the tau protein that can be phosphorylated by Cdk5. The hyperphosphorylation of these sites has been associated with Alzheimer's disease (Yamaguchi et al., 1996; Pei et al., 1998). Spinal cord extracts from *SOD1*^{G37R} mice and normal mice were fractionated by sodium dodecyl sulfate-polyacrylamide gel electrophoresis (SDS-PAGE) followed by immunoblotting with AT-8 or PHF-1 antibodies. No AT-8 and PHF-1 immunoreactivities were detected in samples from normal mice (Figure 2A, lanes 1 and 2, and 2C, lanes 1 and 2). However, in extracts from *SOD1*^{G37R} mice, the AT-8 and PHF-1 antibodies recognized 52–55 kDa species of tau and to a lower extent the 68 kDa species, indicating a hyperphosphorylation of tau in these extracts (Figure 2A, lanes 3 and 4, and 2C, lanes 3 and 4). Alkaline phosphatase treatment of the blot completely abolished the AT-8 and PHF-1 signals for the *SOD1*^{G37R} samples, confirming that the immunoreactivity reflected tau hyperphosphorylation state (data shown later in this article). We have also tested the Tau 1 antibody that recognizes a dephosphorylated epitope of tau at amino acids 191–224 (Iqbal and Grunke-Iqbal, 1995). This epitope includes three Cdk5 recognition sites (Ser 199, Ser 202, and Thr 205) (Baumann et al., 1993; Lew et al., 1995). In extracts from normal mice, the Tau 1 antibodies recognized hypophosphorylated species of tau, including 52–55 kDa, 68 kDa, and 100 kDa bands (Figure 2D, lanes 1 and 2). The signal intensity for Tau 1 immunoreactivity was considerably reduced in samples from the *SOD1*^{G37R} mice (Figure 2D, lanes 3 and 4), confirming an hyperphosphorylation of tau in these extracts. As expected, the Tau 1 signal in *SOD1*^{G37R} samples was restored by alkaline phosphatase treatment of the blots (data shown later in this article; Figure 6). These combined results with the three anti-tau antibodies indicate that tau is hyperphosphorylated in spinal cord of *SOD1*^{G37R} mice.

Table 1. Lifespan of SOD1^{G37R} Mice (lines 29 and 42) with Altered NF Background

Genotype	Average Lifespan (Weeks)	Median of Life Probability (Weeks)*
No perikaryal NF swellings		
SOD1^{G37R} (line 29) (n=40)	51.8 ± 2.1	52.5
SOD1^{G37R} (line 29);*H$^{-/-}$* (n=15)	50.5 ± 2.0	52.0
SOD1^{G37R} (line 42) (n=20)	23.6 ± 1.5	24.0
With perikaryal NF swellings		
SOD1^{G37R} (line 29);*L$^{-/-}$* (n=25)	62.3 ± 5.3	62.8
SOD1^{G37R} (line 29);*hNF-H^{43}* (n=12)	66.0 ± 5.5	68.0
SOD1^{G37R} (line 42);*hNF-H^{43}* (n=7)	24.3 ± 2.2	25.0

*The median of life probability is defined as the age at which the probability of survival is 50%.

In addition, the AT-8 antibodies were used for immunohistochemical staining to confirm the presence of hyperphosphorylated tau in spinal motor neurons of *SOD1^{G37R}*. At the end stage of disease in *SOD1^{G37R}* mice, some motor neurons (20%) in L5 spinal cord sections exhibited intense staining with the AT-8 antibody (Figure 2B, right panel). In contrast, motor neurons from normal mice were poorly stained with the AT-8 antibody (Figure 2B, left panel). The NF-H and NF-M proteins were also abnormally hyperphosphorylated in the *SOD1^{G37R}* mice. In normal mice, insignificant perikaryal staining occurs with the SMI 31 and NN 18 antibodies that recognized the hyperphosphorylated forms of NF-H and NF-M, respectively (Figure 2E, two upper panels). In contrast, in *SOD1^{G37R}* mice, a robust immunostaining of neuronal perikarya was obtained in cell body of motor neurons, demonstrating the abnormal hyperphosphorylation of NF-H and NF-M proteins (Figure 2E, two lower panels).

Alleviation of Disease by Perikaryal Accumulations of NF Proteins

We reported previously that overexpression of human NF-H (hNF-H), a protein containing 34 consensus phosphorylation sites for Cdk5, extended substantially the life span of *SOD1^{G37R}* mice (line 29). Remarkably, a more efficient protection was conferred by the NF-H^{43} allele that produced more prominent NF accumulations in perikarya (Couillard-Després et al., 1998). To investigate further the effects of NF organization and distribution on SOD1-mediated disease, we generated crosses between *SOD1^{G37R}* mice and mice in which the NF-H or NF-L gene had been deleted (respectively, *G37R;H$^{-/-}$* and *G37R;L$^{-/-}$* mice). This was done by breeding procedures with previously described NF-H and NF-L knockout mice (Zhu et al., 1997; Zhu et al., 1998). The disruption of NF-H and NF-L genes in the *SOD1^{G37R}* background produced distinct morphological changes caused by differences in NF protein levels and organization (Figure 3B). Examination at light microscopy of the L5 ventral root at presymptomatic stage (4 months old) showed an hypotrophy of axons presumably due to NF scarcity in the *G37R;L$^{-/-}$* mice, whereas no important changes in axonal caliber occurred in the *G37R;H$^{-/-}$* mice (Figure 3B). Moreover, the motor neurons of *G37R;L$^{-/-}$* exhibited perikaryal swellings caused by NF-H and NF-M subunit accumulations, whereas motor neurons of *G37R;H$^{-/-}$* had normal appearance (Figure 3B). Even though the absence of NF-L provoked an ~90% reduction of NF-H and NF-M protein levels in nervous tissue, an accumulation of these unassembled NF subunits was detected in the perikaryon of motor neurons (Figures 3B and 3C). NF-L is a requirement for the IF assembly and for the efficient transport of newly synthesized NF-M or NF-H proteins (for review, see Lee and Cleveland, 1996; Julien, 1999).

The knockout of NF-H gene did not provoke perikaryal accumulations, and it had no effects on the longevity of *SOD1^{G37R}* (Table 1). In contrast, the absence of NF-L extended the average life span of *SOD1^{G37R}* mice by ~10 weeks. These studies with various *SOD1^{G37R}* mouse lines having NF abnormalities suggested beneficial effects of perikaryal accumulations of NF proteins in disease caused by mutant SOD1.

Because NF-M and NF-H proteins are major Cdk5 substrates with multiple phosphorylation sites, we thought that perikaryal NF accumulations could confer protection by acting as a phosphorylation sink for deregulated Cdk5 activity. Here, we present many lines of evidence that support this model. First, perikaryal NF inclusions in *SOD1^{G37R}* mice were detected with antibodies against hyperphosphorylated NF proteins and that Cdk5 complexes colocalize with these inclusions. Second, the occurrence of perikaryal NF accumulations in *SOD1^{G37R}* mice was found to be associated with reduced phosphorylation of tau, another p25/Cdk5 substrate. Third, there is a correlation between the levels of Cdk5 activity and the longevity of mice expressing different amounts of mutant *SOD1^{G37R}*. Moreover, the perikaryal NF accumulations were found to be less protective in *SOD1^{G37R}* mice that exhibit exceedingly high levels of deregulated Cdk5 activity.

Cdk5 and p25 Colocalize with Perikaryal NF Accumulations in *SOD1^{G37R}* Mice

As shown in Figures 3 and 4, the perikaryal NF accumulations in mice expressing mutant SOD1 in NF-L knockout background or in hNF-H transgenic background are immunoreactive for antibodies recognizing phosphorylated NF proteins. Cdk5 was also immunodetected in cytoplasmic accumulations of NF proteins in spinal motor neurons of 1-year-old *SOD1^{G37R}* mice overexpressing human NF-H (*G37R;hNF-H*) or lacking NF-L gene (*G37R;L$^{-/-}$*) (Figures 4A and 4B). Moreover, immunostaining with antibodies recognizing both p35 and p25 (C-19) revealed a cytoplasmic and perinuclear staining (Figure 4C). Such abnormal localization is likely the result of p25 immunostaining because p35 is normally distributed in the membrane and nerve terminal (Nikolic et al.,

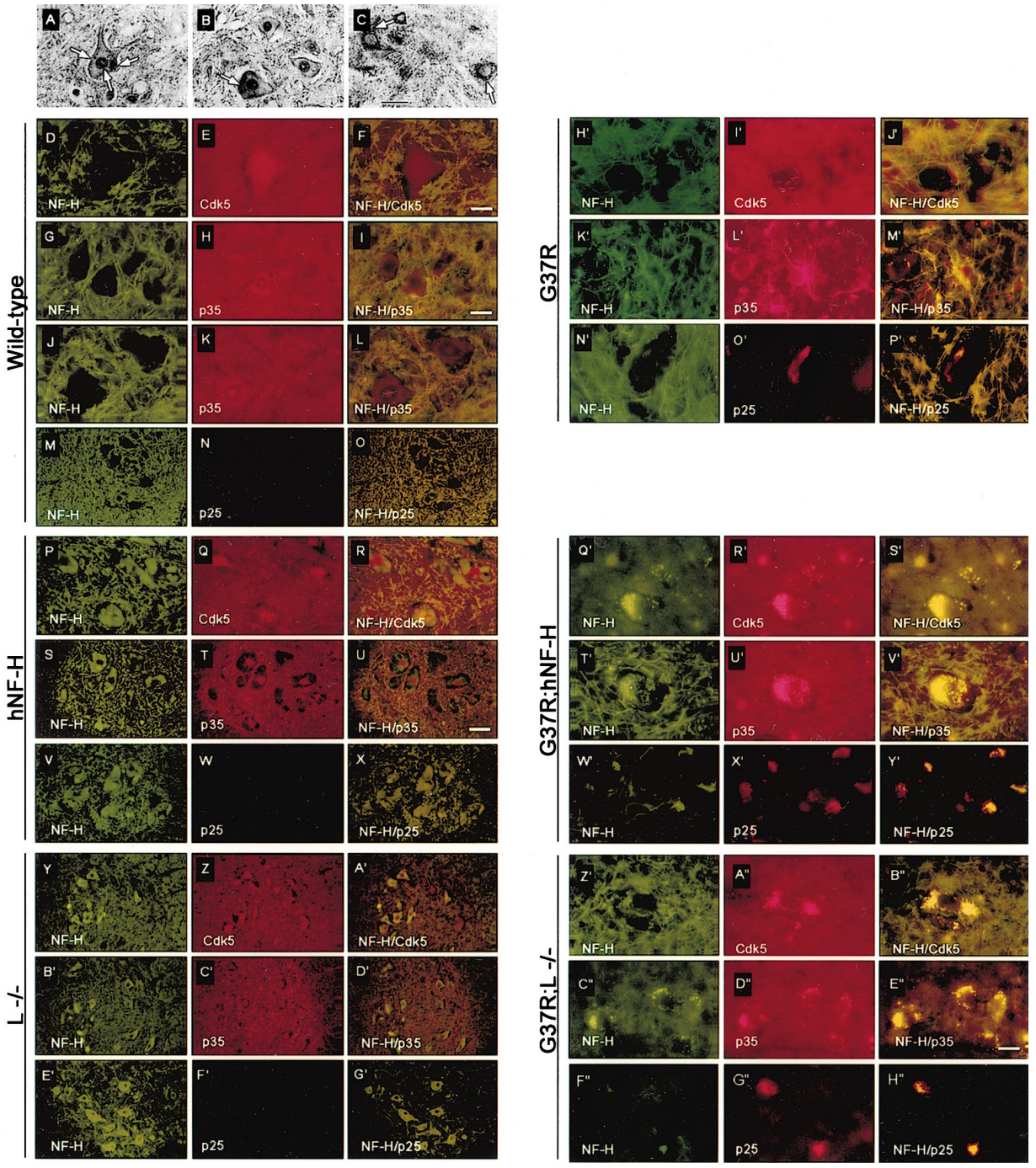

Figure 4. Colocalization of Cdk5 and p25 with Perikaryal Accumulations of NF Proteins in *SOD1*^{G37R} Mice Overexpressing hNF-H or Lacking NF-L

Cdk5 was immunodetected in perikaryal swellings, nucleus, and peripheral membranes of 1-year *SOD1*^{G37R} mice overexpressing *hNF-H*^{44} (A, white arrows) or lacking NF-L (B, white arrows). Mislocalization of the Cdk5 activator p25 in cytoplasmic and perinuclear regions of spinal motor neurons from *G37R;NF-H*^{44}, as revealed with C-19 antibody (C, white arrow). Double immunofluorescence experiments confirmed the colocalization of p25/p35 and Cdk5 with perikaryal accumulations of NF proteins (Q′ to H″), whereas p25/p35 and Cdk5 did not colocalize with hyperphosphorylated NF-H in cell bodies of normal mice (D–O), hNF-H transgenic mice (P–X) and NF-L null mice (Y–G′). In *G37R* mice with a wild-type NF background, the colocalization of Cdk5 and its activators with hyperphosphorylated NFs was sometimes observed (H′ to P′). For instance, (N′) to (P′) show the colocalization of p25 with some perikaryal phosphorylated NF-H. Immunofluorescence experiments on (J) to (L) were performed with the N-20 antibodies that recognize specifically the N terminus of p35 but not p25, whereas p25/p35 immunoreactivities on (H), (I), (T), (U), (C′), (D′), (L′), (M′), (U′), (V′), (D″), and (E″) were obtained with the C-19 antibodies that recognize both p25 and p35. (N), (O), (W), (X), (F′), (G′), (O′), (P′), (X′), (Y′), (G″), and (H″) were obtained with a p25-specific antibody. The NF-H protein was detected with RT-97 and a secondary FITC-labeled antibody, whereas Cdk5, p25, and p35 were detected with a secondary Rhodamine-labeled antibody. Bars: (A–C), 50 μm; (D–F, J–L, H′–P′), 7 μm; (G–I, M–O, P–R, V–X, Q′–V′, Z′–E″), 20 μm; (S–U, Y–G′, W′–Y′, F″–H″), 30 μm.

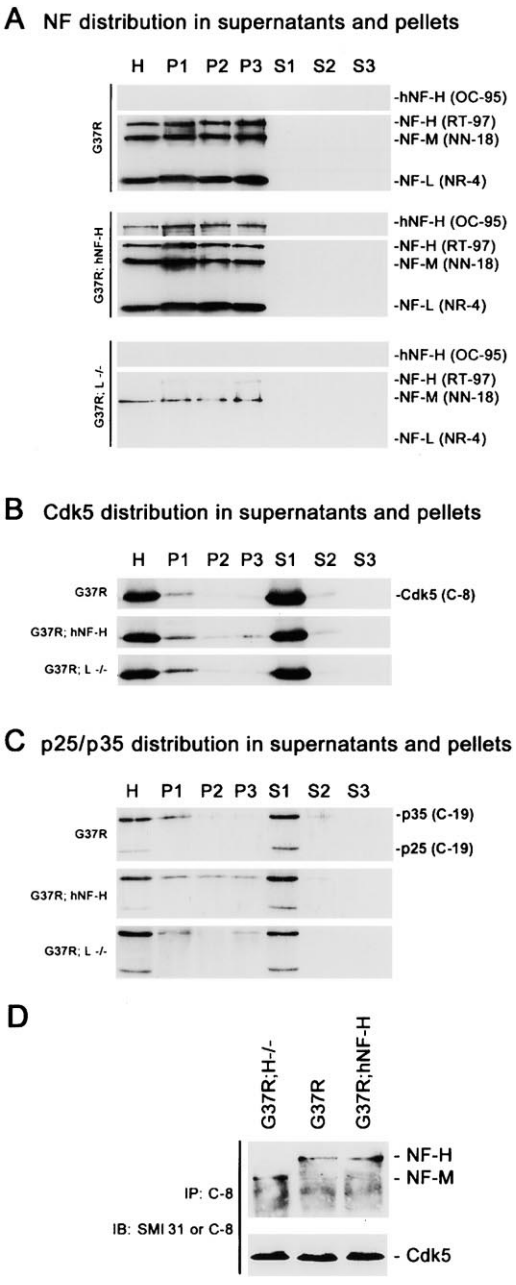

Figure 5. Distribution of NF, p25, p35 and Cdk5 Proteins in Spinal Cord Preparations

(A) Western blots showing the distribution of NF proteins in pellet 1 (P1), P2, and P3 from *SOD1*^{G37R} mice and *SOD1*^{G37R} mice overexpressing hNF-H or lacking NF-L (*G37R*, *G37R;hNF-H*, *G37R;L*$^{-/-}$). Through centrifugation, the NF proteins were recovered mainly in the P1, P2, and P3 fractions. The OC-95 antibodies recognize specifically the human hNF-H protein. Note the considerable decrease in levels of NF proteins from *G37R;L*$^{-/-}$.

(B) Increased levels of Cdk5 recovered in P1 of *G37R;hNF-H* and *G37R;L*$^{-/-}$ mice as compared with P1 of *G37R* mice.

(C) Recovery of p25 in the supernatant 1 (S1) fraction. This suggests that p25 is not sequestered in perikaryal NF inclusions. These results also show that neither overexpression of hNF-H nor lack of NF-L impeded cleavage of p35 to p25 in *SOD1*^{G37R} mice.

(D) Immunoprecipitation of cytoskeletal-enriched fraction from the spinal cord with Cdk5 antibodies (C-8) pulls down phosphorylated NF-H (as detected by SMI 31 antibody) in samples from *G37R* and *G37R;hNF-H* mice but not in sample from *G37R;H*$^{-/-}$ mice. Note that SMI 31 cross-reacts with hyperphosphorylated NF-M in Cdk5 immunoprecipitates from *G37R;H*$^{-/-}$ mice. The membrane was stripped and reprobed with anti-Cdk5 antibodies for the to detection of Cdk5.

1996; Patrick et al., 1999). Moreover, p25 is an abundant Cdk5 coactivator in the spinal cord of *SOD1*^{G37R} mice (Figures 1B, 1C, and 5C). Double immunofluorescence microscopy confirmed the colocalization of Cdk5 and its activators p25, p35 with perikaryal NF protein accumulations in the *G37R*;hNF-H[44] (Figures 4, panels Q′–Y′), and *G37R;L*$^{-/-}$ mice (Figures 4, panels Z′–H″).

Such colocalization of perikaryal NF proteins with Cdk5/activators was not observed in spinal cord sections from normal mice (Figures 4D–4O), hNF-H transgenic mice (Figure 4P–4X) and NF-L null mice (Figure 4Y–4G′). In *SOD1*^{G37R} mice with normal NF background, the codetection of p25, p35, and Cdk5 with phosphorylated NF-H in neuronal cell bodies was sometimes observed (Figure 4, panels H′–P′), but not to the same extent as in *SOD1*^{G37R} mice with perikaryal NF accumulations (Figure 4 Q′–H″). We estimated that ~30% of motor neurons in L5 spinal cord of *SOD1*^{G37R} mice showed perikaryal colocalization of p25/Cdk5 with phosphorylated NF-H. In contrast, the majority of spinal motor neurons in *G37R;L*$^{-/-}$ mice (~70%) and in *G37R;hNF-H* mice (90%) showed colocalization of p25/Cdk5 with phosphorylated NF-H in their perikaryon. Immunostaining of spinal cord sections from the *G37R;hNF-H* or *G37R;L*$^{-/-}$ mice with antibodies against other kinases, including MEK1/2, Erk1/2, JNK, p38, Gsk-3β, and p70S6K did not show colocalization of these kinases with perikaryal NF inclusions (data not shown). The one exception was JNK that was found to localize to small-rounded intracellular inclusions distinct from the perikaryal NF inclusions in *G37R*, *G37R;hNF-H*, and *G37R;L*$^{-/-}$ mice (data not shown).

Following the method of graded centrifugation described previously by Veeranna et al. (2000), we analyzed the distribution of NF, Cdk5, p25, and p35 proteins in different pellets (P) and supernatants (S) (discussed previously in this article). Briefly, protein extracts from the spinal cord of normal and *SOD1*^{G37R} mice were differentially separated by centrifugation (P1 to P3, S1 to S3). These extracts were then fractionated by SDS-PAGE followed by immunoblotting using specific antibodies. Figure 5A shows the levels and distribution of NF proteins in fractions from *SOD1*^{G37R} mice (*G37R*), *G37R*;hNF-H, and *G37R;L*$^{-/-}$ mice. Note that the *G37R;L*$^{-/-}$ mice exhibit a considerable reduction in levels of NF-M and NF-H. In all mice, the NF proteins were recovered essentially in P1, P2, and P3 fractions, whereas Cdk5 was recovered in both P1 and S1 fractions. It is noteworthy that the Cdk5 levels in P1 of *G37R;hNF-H* and *G37R;L*$^{-/-}$ mice were 2- to 3-fold higher than those detected in P1 fraction of single *SOD1*^{G37R} transgenic mice (Figure 5B), suggesting enhanced interactions between Cdk5 and NF proteins in *SOD1*^{G37R} mice with perikaryal NF inclusions.

Further support for the existence of interactions between Cdk5 and NF proteins was provided from immunoprecipitation of Cdk5 with the C-8 antibodies. As

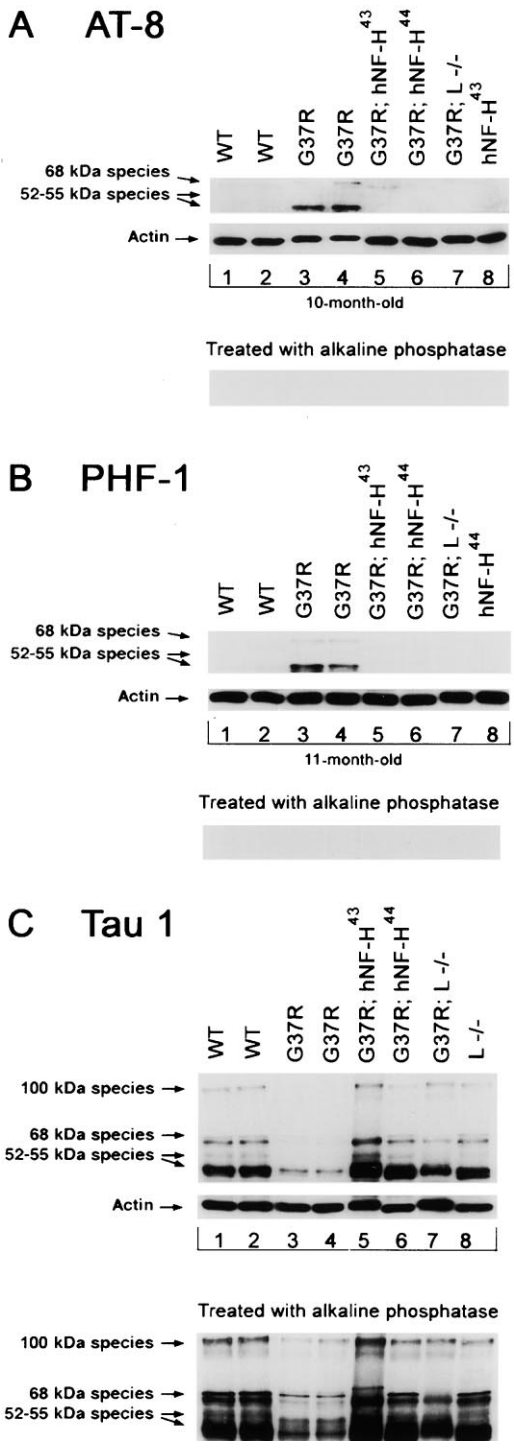

Figure 6. Reduction of Tau Hyperphosphorylation at Cdk5 Sites in *SOD1*^{G37R} Mice Exhibiting Perikaryal NF Accumulations

(A) Western blots using the AT-8 monoclonal antibody indicate alleviation of tau phosphorylation by Cdk5 in *SOD1*^{G37R} mice overexpressing hNF-H transgenes or lacking NF-L. The hyperphosphorylation of tau as indicated by AT-8 immunoreactivities was observed in spinal cord samples of *SOD1*^{G37R} mice (*G37R)* (lanes 3 and 4) unlike normal mice (WT) (lanes 1and 2) and hNF-H transgenic mice (hNF-H) (lane 8). A considerable reduction in AT-8 signals was observed in *SOD1*^{G37R} littermates having perikaryal accumulations of NF proteins, such as *SOD1*^{G37R} mice coexpressing *hNF-H*^{43} (lane 5), *hNF-H*^{44} (lane 6), or lacking NF-L (lane 7).

(B) Attenuation of PHF-1 immunoreactivities in *SOD1*^{G37R} mice with perikaryal NF accumulations. Hyperphosphorylation of tau species as indicated by increased PHF-1 immunoreactivities was observed in spinal cord samples of *SOD1*^{G37R} mice (lanes 3 and 4). There was considerable reduction in PHF-1 signal in samples from *SOD1*^{G37R} littermates exhibiting perikaryal accumulations of NF proteins (lanes 5–7).

(C) Restoration of Tau 1 immunoreactivity in *SOD1*^{G37R} mice overexpressing hNF-H transgenes or lacking NF-L. Hyperphosphorylation of tau as reflected by reduced Tau 1 immunoreactivities occurred in spinal cord samples of *SOD1*^{G37R} mice (lanes 3 and 4). The Tau 1 signals were enhanced in *SOD1*^{G37R} littermates with perikaryal accumulations of NF proteins (lanes 5–7). Treatment of membranes with alkaline phosphatase abolished the AT-8 and PHF-1 signals and enhanced the Tau 1 signals in *SOD1*^{G37R} mice, demonstrating that the signal intensities reflected the tau phosphorylation states rather than tau protein levels.

shown in Figure 5D, the anti-Cdk5 antibodies pulled down phosphorylated NF-H in spinal cord extracts from *SOD1*^{G37R} and *G37R;hNF-H* mice. Moreover, in extracts from *SOD1*^{G37R} mice lacking NF-H (*G37R;H*$^{-/-}$), the anti-Cdk5 antibodies immunoprecipitated hyperphosphorylated NF-M species, as detected with SMI 31 antibodies. The cross-reactivity of SMI 31 with hyperphosphorylated NF-M is a phenomenon that was reported previously in NF-H null mice (Zhu et al., 1998).

The majority of p35 and p25 was recovered in the soluble S1 fraction (Figure 5C). Note that the p25/p35 ratio in the H and S1 fractions from *SOD1*^{G37R} mice (0.5 ± 0.2) was identical to the ratio in samples from *G37R;hNF-H* and *G37R;L*$^{-/-}$ mice (0.5 ± 0.1). Therefore, we conclude that the protective effect of perikaryal NF inclusions in *SOD1*^{G37R} mice does not result from a decrease of p35 cleavage to p25.

Perikaryal NF Proteins Attenuates Tau Phosphorylation

By immunoblotting, we have examined whether the occurrence of perikaryal NF inclusions in lines of *SOD1*^{G37R} mice resulted in a decrease in phosphorylation of tau, another substrate of p25/Cdk5. As shown in Figure 6, the AT-8 and PHF-1 immunoreactivities selective for hyperphosphorylated tau were abolished in spinal cord samples of *SOD1*^{G37R} mice (10 to 12 months old) that exhibited perikaryal accumulations of NF proteins, such as in *SOD1*^{G37R} mice bearing *hNF-H*^{43} or *hNF-H*^{44} transgenes (*G37R;hNF-H*$^{43\ or\ 44}$) and in *SOD1*^{G37R} mice lacking NF-L (*G37R;L*$^{-/-}$). Conversely, the Tau 1 immunoreactivity for hypophosphorylated tau at a Cdk5 epitope was considerably enhanced in spinal cord extracts from these mice. Treatment of the membranes with alkaline phosphatase abolished the AT-8 and PHF-1 immunoreactivities and restored the Tau 1 signal. These results support the view that by acting as a phosphorylation sink, perikaryal NF accumulations could interfere with phosphorylation of other Cdk5 substrates. This model of Cdk5-mediated pathogenesis is presented in Figure 8.

Correlation between Cdk5 Activity in *SOD1*^{G37R} Mice and Longevity

We thought that a correlation between Cdk5 activity and severity of disease would provide further evidence for

a Cdk5 involvement in ALS pathogenesis. Therefore, we have compared the levels of Cdk5 activity in two lines of *SOD1*^{G37R} mice (lines 42 and 29) that exhibit different life span (Figure 7 and Table 1). The *SOD1*^{G37R} mice from line 42 and 29, described previously by Wong et al. (1995), overexpress the SOD1 transgene by ~12-fold and ~5-fold, respectively. As shown in Figure 7, the levels of Cdk5 activity in spinal cord extracts were more elevated (2-fold) in mice from line 42 with a longevity of ~24 weeks than in those from line 29 with a life span of ~52 weeks.

To examine the effect of perikaryal NF accumulations on the life span of mice with high levels of Cdk5 activity, we generated doubly transgenic *SOD1*^{G37R}; *hNF-H*^{43} by crossing *SOD1*^{G37R} mice of line 42 with *hNF-H*^{43} mice. The survival curves in Figure 7 revealed that hNF-H overexpression conferred little protection in *SOD1*^{G37R} mice of line 42. The hNF-H transgene slowed down disease progression by ~1 week in *SOD1*^{G37R} mice from line 42, whereas it extended the life span of mice from line 29 by ~16 weeks (Figures 7A and 7C). These combined results are consistent with a Cdk5 contribution to disease, and they suggest that exceedingly high levels of Cdk5 activity could override the benefit of the NF phosphorylation sink.

Discussion

We report here that a deregulation of Cdk5 activity is associated with disease caused by mutant SOD1. Our results revealed a mislocalization of Cdk5 in the cytoplasm of motor neurons, an elevated ratio of p25 to p35, and an increase of Cdk5 activity in *SOD1*^{G37R} mice, models of ALS. The deregulated Cdk5 activity in *SOD1*^{G37R} mice is accompanied by the hyperphosphorylation of tau and NF proteins, as revealed by immunohistochemistry and immunoblots with various phospho-dependent antibodies. A contribution of Cdk5 to neurodegeneration is suggested from our finding of a correlation between Cdk5 activity and longevity of ALS mice and from the slowing down of disease in *SOD1*^{G37R} mice exhibiting perikaryal accumulations of NF proteins. Because NF proteins are major Cdk5 substrates, we propose that perikaryal NF accumulations may confer protection in *SOD1*^{G37R} mice by acting as a phosphorylation sink for deregulated Cdk5 activity, thereby reducing the noxious hyperphosphorylation of other cellular substrates such as tau (Figure 8).

Several lines of evidence support this phosphorylation sink model. First, the perikaryal NF inclusions in *SOD1*^{G37R} mice with hNF-H transgene or NF-L knockout backgrounds were detectable with antibodies against hyperphosphorylated NF proteins. Second, immunofluorescence data revealed a colocalization of Cdk5/activator complexes with these perikaryal NF inclusions. The recovery of a small fraction of Cdk5 with NFs in P1 and the coimmunoprecipitation of NF-H with Cdk5 also support the view that NF aggregates can interact with Cdk5. Third, *SOD1*^{G37R} mice with perikaryal NF accumulations showed reduction in hyperphosphorylation of tau at Cdk5 sites, as judged by immunoblotting with three specific antibodies: AT-8, PHF-1, and Tau 1. Fourth, the hNF-H transgene overexpression conferred less protec-

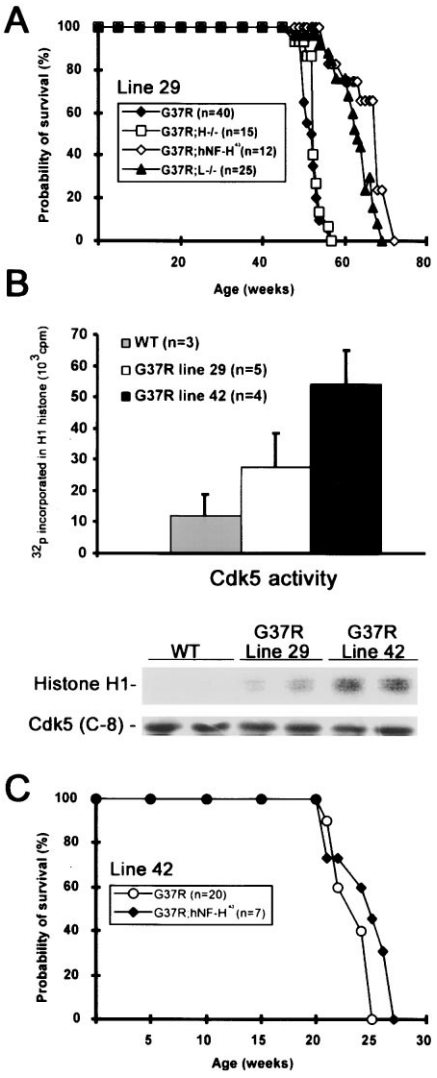

Figure 7. Correlation Between Cdk5 Activity and Longevity of *SOD1*^{G37R} Mice

(A) Survival curves of *SOD1*^{G37R} mice with a normal or altered NF background. The *SOD1*^{G37R} mice (line 29) exhibiting perikaryal NF inclusions as a result of NF-L knockout or overexpression of *hNF-H*^{43} transgene had a lifespan of 10 to 16 weeks longer than *SOD1*^{G37R} mice in normal NF background. The disruption of NF-H gene did not trigger formation of perikaryal NF inclusions, and it had no effect on life span of *SOD1*^{G37R} mice. The survival probability of transgenic mice is plotted as a function of their age in weeks.

(B) Quantification of Cdk5 kinase activity in spinal cord extracts from mice of line 29 overexpressing *SOD1*^{G37R} by 5-fold or from mice of line 42 overexpressing *SOD1*^{G37R} by 12-fold. The kinase assays were performed after immunoprecipitation of extracts with Cdk5 antibodies. The levels of Cdk5 activity were higher in *SOD1*^{G37R} mice of line 42 that have a shorter life span. The autoradiogram shows the quantity of ^{32}P incorporated in histone H1 from Cdk5 in spinal cord extracts of normal and *SOD1*^{G37R} mice (lines 29 and 42) (upper panel) and the levels of Cdk5 immunoprecipitated (lower panel). All kinase assays were carried out using 10-month-old *SOD1*^{G37R} mice (line 29) and 5-month-old *SOD1*^{G37R} mice (line 42).

(C) Survival curves of mice from line 42 expressing *SOD1*^{G37R} in a normal NF background or in a *hNF-H*^{43} transgene background. The hNF-H overexpression slowed down disease by only 1 week in *SOD1*^{G37R} of line 42, suggesting that exceedingly high levels of Cdk5 could override the protective effect of perikaryal NF inclusions.

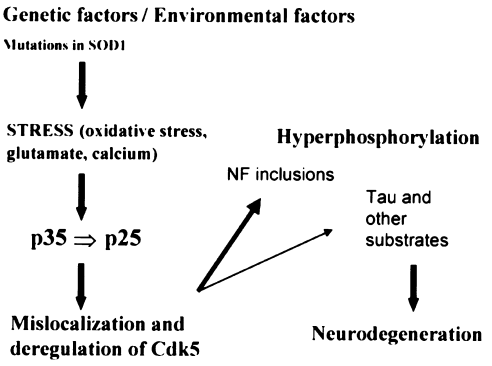

Figure 8. Mechanism of ALS Pathogenesis Due to Deregulated Cdk5 Activity and Protection by Perikaryal NF Inclusions

As a result of changes in calcium homeostasis, the p35 activator can be cleaved by calpain to yield p25 that lacks the myristoylation signal. The mislocalization and deregulation of Cdk5 by p25 promote the hyperphosphorylation of tau with ensuing neurodegeneration. The perikayal NF accumulations act as a phosphorylation sink, and they sequester a fraction of Cdk5, thereby alleviating the noxious hyperphosphorylation of tau and other substrates.

tion in *SOD1^{G37R}* mice (line 42) that exhibit very high levels of Cdk5 activity and early disease onset, suggesting that excess Cdk5 activity could override the NF phosphorylation sink. The use of *SOD1^{G37R}* mouse lines with early-disease onset could explain why no effects on disease progression have been observed with a NF-H-lacZ transgene that induced large perikaryal NF accumulations (Eyer et al., 1998).

It is noteworthy that the occurrence of perikaryal NF inclusions did not affect the ratio of p25 to p35 in *SOD1^{G37R}* mice (Figure 5). Two recent studies showed an induction of p35 cleavage to p25 by the calcium-dependent protease calpain and its inhibition by calpain inhibitors (Kusakawa et al., 2000; Lee et al., 2000). The conversion of p35 to p25 in toxicity of mutant SOD1 is compatible with the current view of altered calcium homeostasis in ALS. A calcium involvement in ALS is strongly supported by the selective vulnerability of motor neurons lacking typical calcium binding proteins, parvalbumin, and calbindin (Ince et al., 1993; Elliot and Snider, 1995), as well as in a line of SOD1 transgenic mice (Morrison et al., 1996). Changes in intracellular calcium could result from oxidative stress and particularly from mitochondrial damage reported in mutant SOD1 transgenic mice (Dal Canto and Gurney, 1995; Wong et al., 1995; Kong and Xu, 1998). Moreover, the overexpression of the calcium binding protein calbindin D_{28K} was recently reported to confer protection against mutant SOD1-mediated death of PC12 cells (Ghadge et al., 1997) and of cultured motor neurons expressing mutant *SOD1^{G93A}* (Roy et al., 1998).

Our findings of deregulated Cdk5 and tau hyperphosphorylation in motor neurons of *SOD1^{G37R}* mice raises up the possibility that tau abnormalities may contribute to ALS pathogenesis. The microtubule-associated protein tau has been implicated in the pathogenesis of neurodegenerative diseases, including Alzheimer's disease and diseases known as tauopathies such as fronto-temporal dementia, ALS/parkinsonism-dementia complex, and progressive supranuclear palsy. Recent studies with transgenic mice overexpressing the shortest human tau isoform demonstrated that neurodegenerative disease can result from tau abnormalities (Ishihara et al., 1999). In addition, the hyperphosphorylation of tau by overexpression of the Cdk5 activator p25 was shown to impair the microtubule-stabilizing function of tau resulting into disruption of the neuronal cytoskeleton (Patrick et al., 1999; Ahlijanian et al., 2000). It should be noted that we did not detect filamentous tau aggregates in *SOD1^{G37R}* mice. Nevertheless, the hyperphosphorylation of tau can reduce its affinity for microtubules resulting in their destabilization. A loss of microtubules can impair axonal transport. Indeed, a slowing of axonal transport has been reported in motor neurons of transgenic mice expressing SOD1 mutants (Zhang et al., 1997; Williamson and Cleveland, 1999).

While recent studies suggest that a deregulation of Cdk5 activity can induce cytoskeletal abnormalities and neuronal death (Patrick et al., 1999; Ahlijanian et al., 2000), more experiments will be needed to determine exactly the degree to which Cdk5 contributes to ALS pathogenesis and to establish the NF phosphorylation sink model. For instance, transfection studies with p25/Cdk5 cDNAs in cultured motor neurons would be useful to confirm further the protective effects of perikaryal NF accumulations and to show that excess Cdk5 activity can override this protection. So far, this approach has been hampered by the absence of perikaryal NF inclusions in cultured motor neurons derived from hNF-H transgenic mice. Thus, more work is required to set up appropriate in vitro culture cell systems. Additional transgenic mouse studies, such as the generation of mice expressing mutant SOD1 in backgrounds of p25 overexpression, p35 knockout, or conditional Cdk5 knockout, would help to resolve fully the role of Cdk5 activity in the neurodegenerative process. An alternative approach of potential relevance for the development of therapy would be the testing of inhibitors of Cdk5 activity for their ability to slow down disease in ALS mice.

Experimental Procedures

Generation and Genotyping of *SOD1^{G37R}* Mouse Lines

Transgenic mice expressing *SOD1^{G37R}* (lines 29 and 42; *G37R*) (Wong et al., 1995), NF-H knockout (*H$^{-/-}$*) mice (Zhu et al., 1998), NF-L knockout mice (*L$^{-/-}$*) (Zhu et al. 1997), and human NF-H^{43} an NF-H^{44} transgenic mice (lines 200 and 1398; *hNF-H$^{43\ or\ 44\ +/-}$*) (Côté et al., 1993; Couillard-Després et al., 1998) have been generated as described previously and have been maintained on a pure C57BL6 background. *G37R;H$^{-/-}$* and *G37R;L$^{-/-}$* were obtained by breeding respectively C57BL6 inbred *G37R;H$^{+/-}$* mice or *G37R;L$^{+/-}$* mice with a littermate *H$^{+/-}$* or *L$^{+/-}$* mice to produce the *G37R;H$^{-/-}$* mice or *G37R;L$^{-/-}$* mice. Inbred C57BL6 doubly transgenic *G37R* (line 29);*hNF-H$^{43\ or\ 44+/-}$* and *G37R* (line 42);*hNF-H$^{43+/-}$* were produced by breeding heterozygous *G37R* mice with heterozygous *hNF-H$^{43\ or\ 44}$* mice. All animals were genotyped by Southern blotting. The life span of our *SOD1^{G37R}* mouse (line 29) in a pure C57BL6 background is ~52 weeks. The use of animals and all surgical procedures described in this article were carried out according to *The Guide to the Care and Use of Experimental Animals of the Canadian Council on Animal Care.*

Immunohistochemistry and Immunofluorescence Analysis

Mice were sacrificed by overdose of chloral hydrate, perfused with 0.9% NaCl, and then with fixative (3% v/v glutaraldehyde in phosphate-buffered saline [PBS] buffer [pH 7.4]). Tissues sections were

prepared for embedding in Epon as described by Zhu et al. (1997). Immunohistochemical studies were performed according to Beaulieu et al. (1999) with antibodies against NF-H (SMI 31, 1:5000; Sternberger Inc., Lutherville, MD), NF-M (NN 18, 1:1000; Boehringer Mannheim, Indianapolis, IN), Cdk5 (C-8, 1:1000; Santa Cruz Biotechnology, Santa Cruz, CA), p25 (N-23, 1:500; a kind gift from Dr. K. Ishiguro), p35 (C-19, 1:1000, Santa Cruz Biotechnology), and tau (AT8, 1:500; Innogenetics, Zwijndrecht, Belgium). The immunochemistry staining was developed using a Vector ABC kit (Vector Laboratories Ltd., Burlington, Canada) and SIGMAFAST tablets (Sigma, Oakille, Canada). For immunofluorescence experiments, mice were perfused with 0.9% NaCl and then with fixative (4% v/v paraformaldehyde in PBS buffer [pH 7.4]). Tissue samples were processed according to Beaulieu et al. (1999) with the exceptions of permeabilization buffer (PBS; 10% NGS [v/v], 0.2% Triton X-100 [v/v]), 0.2% (v/v), and the blockade solution (PBS, 2% NGS [v/v], 0.05% [v/v] Triton X-100). Tissues samples were incubated with antibodies against NF-H (RT97, 1:500; Boehringer Mannheim), NF-M (NN 18, 1:100), Cdk5 (C-8, 1:100), and p35 (C-19, 1:100; N-20, 1:100; Santa Cruz Biotechnology).

Immunoprecipitation and Kinase Assays

Spinal cord tissues were extracted from mice and homogenized in lysis buffer (20 mM Tris [pH 8.0], 137 mM NaCl, 10% glycerol, 1% NP40, 1 μg/ml leupeptin, 10 μg/ml apoprotinin, and 0.5 mM sodium orthovanadate and 1mM phenylmethylsulfonyl fluoride [PMSF]). Histone H1 kinase assay was carried according to Tsai et al. (1993) with 250 μg of spinal cord lysates.

Western Blot Analysis and Alkaline Phosphatase Treatment

The mice were sacrificed by intraperitoneal injection of chloral hydrate. Immediately after, total protein extracts were obtained by homogenization in SDS-urea β-mercaptoethanol (0.5% SDS, 8 M urea in 7.4 phosphate buffer) with a cocktail of protease inhibitors (PMSF, leupeptin, pepstatin, apoprotinin) or in lysis buffer described previously in this article. The protein concentration was estimated by the Bradford procedure (Bio-Rad Laboratories, Hercules, CA). Proteins were fractionated on 7.5% or 10% SDS-PAGE and blotted on a nitrocellulose membrane for Western blot analysis. Membranes were incubated with monoclonal antibodies against NF-L (NR4, 1:1000; Boehringer Mannheim), NF-M (NN-18, 1:1000), NF-H (RT-97, 1:1000, and SMI 31, 1:5000), tau (AT-8, 1:1000; Tau 1, 1:1000; Boehringer Mannheim; PHF-1, 1:100), actin (C-4, 1:5000; Boehringer Mannheim), human SOD1 (1:1000; Biodesign Inc., New York), Cdk5 (C-8, 1:1000; J-3, 1:500; Santa Cruz Biotechnology), and p35 (C-19, 1:1000; N-23, 1:500). The Western blots were revealed by RENAISSANCE, a Western blot chemiluminescence kit from NEN Life Science (Boston, MA). Alkaline phosphatase treatment was performed as described in protocols for tissue dephosphorylation with Tau 1 antibody from Boehringer Mannheim.

Centrifugation of Spinal Cord Extracts

After dissection, the spinal cord samples were used immediately or frozen at −80°C. The preparation of NFs and Cdk5/activator complexes was based on a procedure described by Veeranna et al. (2000). The spinal cords were homogenized in the extraction buffer 1 (25 mM Tris [pH 6.8], 1% Triton X-100, 100 nM NaCl, 1.0 mM EDTA, 2.0 mM EGTA, 5 μg/ ml leupeptin, and 4 mM PMSF). The homogenate (H) was centrifuged at 15,000 g for 1 hr at 4°C, and the supernatant (S1) was saved. The pellet 1 (P1) was resuspended in extraction buffer 2 (buffer 1 with 1.0 M sucrose) and centrifuged at 15,000 g for 35 min at 4°C. The supernatant S2 was saved, and the pellet P2 was again resuspended in buffer 2 and centrifuged for 35 min at 4°C. The supernatant S3 was saved, and the final pellet was resuspended and saved as P3.

Acknowledgments

The technical help of P. Hince, G. Gagnon, J. Laganière, and D. Houle is gratefully acknowledged. We thank Drs. Q. Zhu, J. Robertson, D. R. Kaplan, J.-M. Beaulieu, and M. Boudreau for helpful discussions. We are grateful to Dr. P. Davies for the PHF-1 antibodies, Dr. K. Ishiguro for the p25 N-terminus antibodies, and Drs. D. L. Price and D. W. Cleveland for the kind gift of *SOD1*^{G37R} mice (lines 29 and 42). This work was supported by the ALS Association (USA), the Canadian Institutes of Health Research (CIHR), and the Neuromuscular Research Partnership, an initiative of ALS Canada, MDAC, and CIHR. M. D. N. is a recipient of a CIHR studentship and a K. M. Hunter/CIHR Scholarship. J.-P. J. holds a CIHR Senior Investigator Award.

Received April 21, 2000; revised January 19, 2001.

References

Ahlijanian, M.K., Barrezueta, N.X., Williams, R.D., Jakowski, A., Kowsz, K.P., McCarthy, S., Coskran T., Carlo, A., Seymour, P.A., Burkhardt, J.E., et al. (2000). Hyperphosphorylation of tau and neurofilaments and cytoskeletal disruptions in mice overexpressing human p25, an activator of Cdk5. Proc. Natl. Acad. Sci. USA *97*, 2910–2915.

Bajaj, N.P., and Miller, C.C.J. (1997). Phosphorylation of neurofilament heavy-chain side-arm fragments by cyclin-dependent kinase-5 and glycogen synthase kinase-3α in transfected cells. J. Neurochem. *69*, 737–743.

Bajaj, N.P., Al-Sarraj, S.T., Anderson, V., Kibble, M., Leigh, P.N., and Miller, C.C.J. (1998). Cyclin-dependent kinase-5 is associated with lipofuscin in motor neurons in amyotrophic lateral sclerosis. Neurosci. Lett. *245*, 45–48.

Bajaj, N.P., Al-Sarraj, S.T., Leigh, P.N., Anderson, V., and Miller, C.C.J. (1999). Cyclin dependent kinase-5 (CDK-5) phosphorylates neurofilament heavy (NF-H) chain to generate epitopes for antibodies that label neurofilament accumulations in amyotrophic lateral sclerosis (ALS) and is present in affected motor neurons in ALS. Prog. Neuropsychopharmacol. Biol. Psychiatry *23*, 833–850.

Baumann, K., Mandelkow, E.M., Biernat, J., Piwnica-Worms, H., and Mandelkow, E. (1993). Abnormal Alzheimer-like phosphorylation of tau-protein by cyclin-dependent kinases cdk2 and cdk5. FEBS Lett. *336*, 417–424.

Beaulieu, J.-M., Nguyen, M.D., and Julien, J.-P. (1999). Late onset death of motor neurons in mice overexpressing wild-type peripherin. J. Cell. Biol. *147*, 531–544.

Beaulieu, J.-M., Jacomy, H., and Julien, J.P. (2000). Formation of intermediate filament protein aggregates with disparate effects in two transgenic mouse models lacking the neurofilament light subunit. J. Neurosci. *20*, 5321–5328.

Beckman, J.S., Carson, M., Smith, C.D., and Koppenol, W.H. (1993). ALS, SOD and peroxynitrite. Nature *364*, 584.

Brion, J.P., and Couck, A.M. (1995). Cortical and brainstem-type lewy bodies are immunoreactive for the cyclin-dependent kinase 5. Am. J. Pathol. *147*, 1465–1476.

Bruijn, L.I., Becher, M.W., Lee, M.K., Anderson, L.L., Jenkins, N.A., Copeland, N.G., Sisodia, S.S., Rothstein, J.D., Borchelt, D.R., Price, D.L., and Cleveland, D.W. (1997). ALS-linked SOD1 mutant G85R mediates damage to astrocytes and promotes rapidly progressive disease with SOD1-containing inclusions. Neuron *18*, 327–338.

Bruijn, L.I., Houseweart, M.K., Kato, S., Anderson, K.L., Anderson, S.D., Ohama, E., Reaume, A.G., Scott, R.W., and Cleveland, D.W. (1998). Aggregation and motor neuron toxicity of an ALS-linked SOD1 mutant independent from wild-type SOD1. Science *281*, 1851–1854.

Carpenter, S. (1968). Proximal axonal enlargement in motor neuron disease. Neurology *18*, 841–851.

Cleveland, D.W. (1999). From Charcot to SOD1: mechanisms of selective motor neuron death in ALS. Neuron *24*, 515–520.

Corson, L.B., Strain, J.J., Culotta, V.C., and Cleveland, D.W. (1998). Chaperone-facilitated copper binding is a property common to several classes of familial amyotrophic lateral sclerosis-linked superoxide dismutase mutants. Proc. Natl. Acad. Sci. USA *95*, 6361–6366.

Côté, F., Collard, J.F., and Julien, J.-P. (1993). Progressive neuropathy in transgenic mice expressing the human neurofilament heavy gene: a mouse model of amyotrophic lateral sclerosis. Cell *73*, 35–46.

Couillard-Després, J.-S., Zhu, Q., Wong, P.C., Price, D.L., Cleveland, D.W., and Julien, J.-P. (1998). Protective effect of neurofilament NF-H overexpression in motor neuron disease induced by mutant superoxide dismutase. Proc. Natl. Acad. Sci. USA *95*, 9626–9630.

Cudkowicz, M.E., McKenna-Yasek, D., Sapp, P.E., Chin, W., Geller, B., Hayden, D.L., Schoenfeld, D.A., Hosler, B.A., Horvitz, H.R., and Brown, R.H. (1997). Epidemiology of mutations in superoxide dismutase in amyotrophic lateral sclerosis. Ann. Neurol. *41*, 210–221.

Dal Canto, M.C., and Gurney, M.E. (1995). Neuropathological changes in two lines of mice carrying a transgene for mutant human Cu,Zn SOD, and in mice overexpressing wild type human SOD: a model of familial amyotrophic lateral sclerosis (FALS). Brain Res. *676*, 25–40.

Elliot, J.L., and Snider, W.D. (1995). Parvalbumin is a marker of ALS-resistant motor neurons. Neuroreport *6*, 449–452.

Estevez, A.G., Crow, J.P., Sampson, J.B., Reiter, C., Zhuang, Y., Richardson, G.J., Tarpey, M.M., Barbeito, L., and Beckman, J.S. (1999). Induction of nitric oxide-dependent apoptosis in motor neurons by zinc-deficient superoxide dismutase. Science *286*, 2498–2500.

Eyer, J., Cleveland, D.W., Wong, P. C., and Peterson, A.C. (1998). Pathogenesis of two axonopathies does not require axonal neurofilaments. Nature *391*, 584–587.

Fridovich, I. (1986). Superoxide dismutases. Adv. Enzymol. Relat. Areas Mol. Biol. *58*, 61–97.

Ghadge, J.D., Lee, J.P., Bindokas, V.P., Jordan, J., Ma, L., Miller, R.J., and Roos, R. (1997). Mutant superoxide dismutase-1-linked familial amyotrophic lateral sclerosis: molecular mechanisms of neuronal death and protection. J. Neurosci. *17*, 8756–8766.

Giasson, B.I., and Mushynski, W.E. (1996). Aberrant stress-induced phosphorylation of perikaryal neurofilaments. J. Biol. Chem. *271*, 30404–30409.

Green, S.L., Vulliet, P.R., Pinter, M.J., and Cork, L.C. (1998). Alterations in cyclin-dependent kinase 5 (CDK5) protein levels, activity and immunocytochemistry in canine motor neuron disease. J. Neuropathol. Exp. Neurol. *57*, 1070–1077.

Guidato, S. Tsai, L.H., Woodgett, J., and Miller, C.C.J. (1996). Differential cellular phosphorylation of neurofilament heavy side-arms by glycogen synthase kinase-3 and cyclin-dependent kinase-5. J. Neurochem. *66*, 1698–1706.

Hirano, A., Nakano, I., Kurland, L.T., Mulder, D.W., Holley, P.W., and Saccomanno, G. (1984). Fine structural study of neurofibrillary changes in a family with amyotrophic lateral sclerosis. J. Neuropathol. Exp. Neurol. *43*, 471–480.

Ince, P., Stout, N., Shaw, P., Slade, J., Hunziker, W., Heizmann, C.W., and Baimbridge, K.G. (1993). Parvalbumin and calbindin D-28K in the human motor system and in motor neuron disease. Neuropathol. Appl. Neurobiol. *19*, 291–299.

Iqbal, K., and Grundke-Iqbal, I. (1995). Alzheimer abnormally phosphorylated tau is more hyperphosphorylated than the fetal tau and causes the disruption of microtubules. Neurobiol. Aging *16*, 375–379.

Ishihara, T., Hong, M., Zhang, B. Nakagawa, Y., Lee, M.K., Trojanowski, J.Q., and Lee, V.M. (1999). Age-dependent emergence and progression of a tauopathy in transgenic mice overexpressing the shortest human tau isoform. Neuron *24*, 751–762.

Julien, J.-P. (1999). Neurofilament functions in health and disease. Curr. Opin. Neurobiol. *9*, 554–560.

Julien, J.-P. (2001). Amyotrophic lateral sclerosis: unfolding the toxicity of the misfolded. Cell *104*, 571–591.

Kong J., and Xu, Z. (1998). Massive mitochondrial degeneration in motor neurons triggers the onset of amyotrophic lateral sclerosis in mice expressing a mutant SOD1. J. Neurosci. *18*, 3241–3250.

Kusakawa, G.I., Saito, T., Onuki, R., Ishiguro, K., Kishimoto, T., and Hisanaga, S. (2000). Calpain-dependent proteolytic cleavage of the p35 Cdk5 activator to p25. J. Biol. Chem. *275*, 166–172.

Kwon, Y.T., and Tsai, L.H. (1998). A novel disruption of cortical development in p35 (−/−) mice distinct from reeler. J. Comp. Neurol. *395*, 510–522.

Lee, M.K., and Cleveland, D.W. (1996). Neuronal intermediate filaments. Annu. Rev. Neurosci. *19*, 187–217.

Lee, M.-S., Kwon, Y.T., Li, M., Peng, J., Friedlander, R.M., and Tsai, L.-H. (2000). Neurotoxicity induces cleavage of p35 into p25. Nature *405*, 360–364.

Lew, J. QI, Z., Huang, Q.-Q., Paudel, H., Matsuura, I., Matsushita, M., Zhu, X., and Wang, J.H. (1995). Structure, function, and regulation of neuronal Cdc2-like protein kinase. Neurobiol. Aging *16*, 263–270.

Li, M., Ona, V.O., Guégan, C., Chen, M., Jackson-Lewis, V., Andrews, L.J., Olzewski, A.J., Stieg, P.E., Lee, J.P., Przedborski, S., and Friendlander, R.M. (2000). Functional role of caspase-1 and caspase-3 in an ALS transgenic mouse model. Science *288*, 335–339.

Mandelkow, E. (1999). The tangled tale of tau. Nature *402*, 588–599.

Morrison, B.M., Gordon, J.W., Ripps, M.E., and Morrison, J.H. (1996). Quantitative immunocytochemical analysis of the spinal cord in G86R superoxide dismutase transgenic mice: neurochemical correlates of selective vulnerability. J. Neurol. Comp. *373*, 619–631.

Nikolic, M., Dudek, H., Kwon, Y.T., Ramos, Y.F., and Tsai, L.H. (1996). The cdk5/p35 kinase is essential for neurite outgrowth during neuronal differentiation. Genes Dev. *10*, 816–825.

Oshima T., Ward, J.M., Huh, C.G., Longenecker, G., Veeranna G.J., Pant, H.C., Brady, R.O., Martin, L.J., and Kulkarni, A.B. (1996). Targeted disruption of the cyclin-dependent kinase 5 gene results in abnormal corticogenesis, neuronal pathology and perinatal death. Proc. Acad. Natl. Sci. USA *93*, 11173–11178.

Pasinelli, P., Borchelt, D.R., Houseweart, M.K., Cleveland, D.W., and Brown, R.H., Jr. (1998). Caspase-1 is activated in neural cells and tissue with amyotrophic lateral sclerosis-associated mutations in copper-zinc superoxide dismutase. Proc. Natl. Acad. Sci. USA *95*, 15763–15768.

Patrick, G.N., Zukerberg, L., Nikolic, M., de la Monte, S., Dikkes, P., and Tsai, L.H. (1999). Conversion of p35 to p25 deregulates Cdk5 activity and promotes neurodegeneration. Nature *402*, 615–622.

Pei, J.J., Grundke-Iqbal, I., Iqbal, K., Bogdanovic, N., Winblad. B., and Cowburn, R.F. (1998). Accumulation of cyclin-dependent kinase 5 (cdk5) in neurons with early stages of Alzheimer's disease neurofibrillary degeneration. Brain Res. *797*, 267–277.

Rosen, D.R., Siddique, T., Patterson, D., Figlewicz, D.A., Sapp, P., Hentati, A., Donaldson, D., Goto, J., O'Reagan, J.P., Deng, H.-X., et al. (1993). Mutation in Cu/Zn superoxide dismutase gene are associated with familial amyotrophic lateral sclerosis. Nature *362*, 59–62.

Rouleau, G.A., Clarke, A.W., Rooke, K., Pramatarova, A., Krizus, A., Suchowersky, O., Julien, J.-P., and Figlewicz, D.A. (1996). SOD1 mutation is associated with accumulations of neurofilaments in amyotrophic lateral sclerosis. Ann. Neurol. *39*, 128–131.

Roy, J., Minotti, S., Dong, L., Figlewicz, D.A., and Durham, H.D. (1998). Glutamate potentiates the toxicity of mutant Cu/Zn-superoxide dismutase in motor neurons by postsynaptic calcium-dependent mechanisms. J. Neurosci. *18*, 9673–9684.

Schmidt, M.L., Carden, M.J., Lee, V.M., and Trojanowski, J.Q. (1997). Phosphate dependent and independent neurofilament epitopes in the axonal swellings of patients with motor neuron disease and controls. Lab. Invest. *56*, 282–294.

Trotti, D., Rolfs, A., Danbolt, N.C., Brown Jr., R.H., and Hediger, M.A. (1998). SOD1 mutants linked to amyotrophic lateral sclerosis selectively inactivate a glial glutamate transporter. Nat. Neurosci. *2*, 427–433.

Tsai, L.H., Takahashi, T., Caviness, V.S., Jr., and Harlow, E. (1993). Activity and expression pattern of cyclin-dependent kinase 5 in the embryonic mouse nervous system. Development *119*, 1029–1040.

Tsai, L.H., Delalle, I., Caviness, V.S., Jr., Chae, T., and Harlow, E. (1994). P35 is a neural-specific regulatory subunit of cyclin-dependent kinase 5. Nature *371*, 419–423.

Veeranna, G.J., Amin, N.D., Ahn, N.G., Jaffe, H., Winters, C.A., Grant, P., and Pant, H.C. (1998). Mitogen-activated protein kinases (Erk1, 2) phosphorylate Lys-Ser-Pro (KSP) repeats in neurofilament proteins NF-H and NF-M. J. Neurosci. *18*, 4008–4021.

Veeranna, G.J., Shetty, K.T., Takahashi, M., Grant, P., and Pant,

H.C. (2000). Cdk5 and MAPK are associated with complexes of cytoskeletal proteins in rat brain. Mol. Brain Res. *76*, 229–236.

Wideau-Pazos, M., Goto, J.J., Rabizadeh, S., Gralla, E.B., Roe, J.A., Lee, M.K., Valentine, J.S., and Bredesen, D.E. (1996). Altered reactivity of superoxide dismutase in familial amyotrophic lateral sclerosis. Science *271*, 515–518.

Williamson, T.L., and Cleveland, D.W. (1999). Slowing of axonal transport is a very early event in the toxicity of ALS-linked SOD1 mutants to motor neurons. Nat. Neurosci. *2*, 50–56.

Williamson, T.L., Bruijn, L.I., Zhu, Q., Anderson, K.L., Anderson, S.D., Julien, J.P., and Cleveland, D.W. (1998). Absence of neurofilaments reduces the selective vulnerability of motor neurons and slows disease caused by a amyotrophic lateral sclerosis-linked superoxide dismutase 1 mutant. Proc. Natl. Acad. Sci. USA *95*, 9631–9636.

Wong, P.C., Pardo, C.A., Borchelt, D.R., Lee, M.K., Copeland, N.G., Jenkins, N.A., Sisodia, S.S., Cleveland, D.W., and Price, D.L. (1995). An adverse property of a familial ALS-linked SOD1 mutation causes motor neuron disease characterized by vacuolar degeneration of mitochondria. Neuron. *14*, 1105–1116.

Yamaguchi, H., Ishiguro, K., Uchida, T., Takashima, A., Lemere, C.A., and Imahori, K. (1996). Preferential labeling of Alzheimer neurofibrillary tangles with antisera for tau protein kinase (TPK)I/glycogen synthase kinase-3 and cyclin-dependent kinase *5*, a component of TPK II. Acta Neuropathol. *92*, 232–241.

Zhang, B., Tu, P., Abtahian, F., Trojanowski, J.Q., and Lee, V.M. (1997). Neurofilaments and orthograde transport are reduced in ventral root axons of transgenic mice that express human SOD1 with a G93A mutation. J. Cell. Biol. *139*, 1307–1315.

Zhu, Q., Couillard-Després, S.-D., and Julien, J.-P. (1997). Delayed maturation of regenerating myelinated axons in mice lacking neurofilaments. Exp. Neurol. *148*, 299–316.

Zhu, Q., Lindenbaum, M., Levavasseur, F., Jacomy, H., and Julien, J.-P. (1998). Disruption of the NF-H gene increases axonal microtubule content and velocity of neurofilament transport: relief of axonopathy resulting from the beta, beta′-iminodiproprionitrile. J. Cell Biol. *143*, 183–193.